NJC

Accepted Manuscript

This is an *Accepted Manuscript*, which has been through the Royal Society of Chemistry peer review process and has been accepted for publication.

Accepted Manuscripts are published online shortly after acceptance, before technical editing, formatting and proof reading. Using this free service, authors can make their results available to the community, in citable form, before we publish the edited article. We will replace this *Accepted Manuscript* with the edited and formatted *Advance Article* as soon as it is available.

You can find more information about *Accepted Manuscripts* in the Information for Authors.

Please note that technical editing may introduce minor changes to the text and/or graphics, which may alter content. The journal's standard Terms & Conditions and the Ethical guidelines still apply. In no event shall the Royal Society of Chemistry be held responsible for any errors or omissions in this *Accepted Manuscript* or any consequences arising from the use of any information it contains.

ROYAL SOCIETY OF CHEMISTRY

www.rsc.org/njc

Catalytic Activity of Anionic Au-Ag Dimer for Nitric Oxide Oxidation: A DFT Study

Debajyoti Bhattacharjee[1], Bhupesh Kumar Mishra[1,2], Arup Kumar Chakrabartty[1] and Ramesh Ch. Deka[1*]

[1]Department of Chemical Sciences, Tezpur University Tezpur, Napaam, 784 028, Assam, India.

[2]Department of Chemistry, D.N. Government College, Itanagar, Arunachal Pradesh-791113, India

[*]Corresponding author. Tel.: +91 3712267008; Fax: +91 3712 267005

E-mail address: ramesh@tezu.ernet.in

Abstract

Bimetallic nanoparticles composed of two different metals such as Au-Ag show novel catalytic behavior based on the effect of second metal element added. Considering this fact, we performed density functional theory (DFT) calculations to study the oxidation pathway of NO promoted by anionic $Au\text{-}Ag^-$ dimer. During our investigations, we have considered two most plausible pathways of NO oxidation. We found that the anionic $Au\text{-}Ag^-$ dimer can effectively catalyze NO oxidation reaction. In $Au\text{-}Ag^-$, the Au site is more active than the Ag site, and the calculated energy barrier values for the rate determining step of the Au-site catalytic reaction are remarkably lower than those for both the Ag-site catalytic reactions. The present results enrich our understanding of the catalytic oxidation of NO by Au-Ag cluster based catalyst. For the first time, we have presented a systematic study on the structure and energetic of various reaction intermediates involved in NO oxidation by $Au\text{-}Ag^-$ dimer using DFT. The T1 diagnostic calculation suggests that the multi-reference character is not an issue for present study.

Key words: $Au\text{-}Ag^-$, NO oxidation, DFT, T1diagnostic

1. Introduction

In recent days, oxides of carbon and nitrogen such as carbon monoxide (CO) and nitrogen oxides (NO_x) found importance due to their contribution towards green house effect.[1-3] These oxides are mainly emitted from automobile exhaust due to incomplete combustion in the engine.[4] Among the oxides of nitrogen, nitric oxide is a free radical, chemically unstable and has a lifetime of 5 seconds. Catalytic conversion of harmful gases, such as the oxides of nitrogen and carbon monoxide into nitrogen and carbon dioxide, is still challenging from both environmental and economical view. They are responsible for global warming which can lead to climate change that causes sea levels to raise, increases salinity in ocean ecosystems, and affects rainfall patterns. In addition to global warming, these substances can adversely affect the living organism. It received considerable attention in the last two decades due to its impacts on the environment such as acid rain and photochemical smog formation.[5,6] Due to the toxic effects of these gases, research is widely going on today for the removal and conversion of these gases mainly using the concept of catalysis. Among different catalysts, precious metals such as Au, Ag, Pd, Pt etc. show potential activity towards the removal of green house gases.[7-9] As a new kind of catalyst to reduce air pollution, nanosized gold clusters have attracted attention in scientific community. The study of Torres *et al*. revealed that Au (111) surface can effectively catalyzed the NO to NO_2.[10] Ding et al. have used DFT to investigate NO molecule adsorption on the gold clusters, observing the strong ability to adsorb NO molecule for the majority of gold clusters.[11] Hakkinen and his group established both theoretically and experimentally that anionic Au_2 dimer is the smallest unit which can catalyze CO oxidation reaction.[9,12] They observed two different pathways for CO oxidation, one involving carbonate like intermediate and other via peroxyformate like intermediate. In

another report, Gao *et al*. [13] performed ab-initio study on catalytic activities of subnanometer gold clusters with particular attention in the size range of Au_{16}-Au_{35}. They found Au_{34} as an electronic magic cluster for CO oxidation with strong CO and O_2 adsorption sites.

In addition to monometallic clusters, bimetallic nanoclusters composed of two different metal elements such as Au-Ag are much more promising because of their synergistic effects. They show novel catalytic behavior based on the effect of second metal element added.[14] Zhao *et al*. performed DFT calculations to study the structural and energetic properties of NO, NO_2 and NO_3 binding on small bimetallic Au_nCu_m clusters ($n + m \leq 5$).[15] They found that NO is adsorbed in atop configuration via the N atom while NO_2 and NO_3 are generally adsorbed in bridge configuration via the O atoms. Peng *et al*. carried out (DFT) calculations to investigate CO and O_2 adsorption as well as CO oxidation on the Au_mPd_n ($m + n = 2–6$) bimetallic clusters.[16] They found that the adsorption energies of both CO and O_2 on Au_mPd_n ($m + n = 2–6$) are greater than those on the pure gold clusters of corresponding sizes, and unexpectedly greater than those on Pd clusters in some cases. Considering the catalytic activity of Au_2^- dimer towards CO oxidation as well as the enhance activity of bimetallic clusters, Liu et al. studied the same reaction catalyzed by Au-Ag^- dimer in the gas phase and compared it with the pure Au_2^- dimer.[17] They found that anionic Au-Ag^- dimer has great catalytic activity for CO oxidation and also the activity is higher compared to that of pure Au_2^- dimer. As Au-Ag^- promotes CO oxidation in the gas phase; it is both natural and promising for us to investigate the catalytic activity of Au-Ag^- towards NO oxidation. Therefore, in this work, we have investigated the catalytic activity of Au-Ag^- dimer towards NO oxidation. Since Au is the most electronegative metal and the polarization effect are usually observed in Au, its alloy nanoparticles supported on substrates leads to the negatively

charged nanoparticles. Thus the anionic clusters are appropriate for mimicking the catalytic reactivities of Au and Au-Ag nanoparticles.[17] To the best of our knowledge, no detailed theoretical or experimental studies have been reported for this reaction. In view of the potential importance and the rather limited information, we carry out a detailed theoretical study on the potential energy surface (PES) of the title reaction to (1) provide the elaborate oxidation channels; (2) investigate the products of the title reaction to assist in further experimental identification; and (3) give deep insight into the mechanism of the reaction of anionic gold-silver dimer with nitrogen oxide. Therefore, to get a more complete picture of the oxidation processes of NO on the anionic Au-Ag dimers, it is pertinent to perform a comprehensive theoretical study to determine the energetics involved in the NO oxidation by considering full structure optimization.

In recent years, density functional theory (DFT) has become a valuable tool for studying the properties of molecules and materials[8,18-20] and for identifying reaction mechanisms.[21,22] In this communication, for the first time, we have presented a systematic study on the structure and energetics of various reaction intermediates involved in NO oxidation by $Au\text{-}Ag^-$ dimer using density functional theory (DFT).

2. Methodology

The focus of our detail study was based on the following reaction.

$$2NO + O_2 \xrightarrow{Au\text{-}Ag^-} 2NO_2$$

For $Au\text{-}Ag^-$ dimer, the reaction branches into the Au-site catalytic series and Ag-site catalytic series. We chose two most plausible pathways for the oxidation of NO during present study as given by path 1 and path 2.

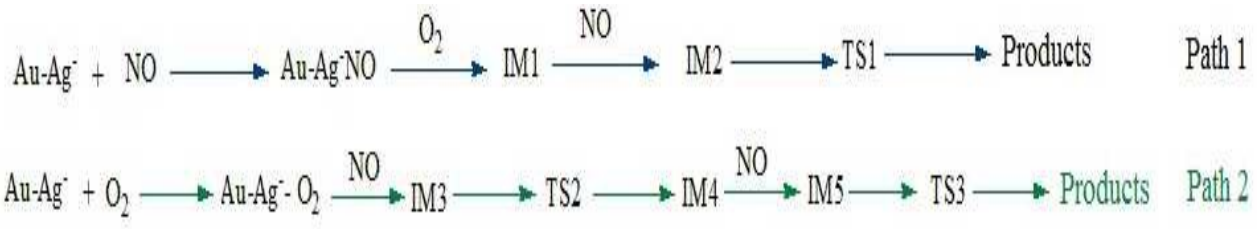

where, IM and Ts stands for intermediate and transition states, respectively. All calculations were performed using Gaussian 09 suits of program.[23] In the frame work of density functional theory (DFT), we employ the hybrid B3LYP[24,25] functional to explore the stationary points on the potential energy surfaces. Considering the strong relativistic effect of Au and Ag, we used the Los Alamos LANL2DZ[26,27] Effective Core Pseudopotentials (ECP) and valence double-ζ basis sets for Au and Ag atoms. The N and O atoms were treated with the 6-311G+(d) basis sets. No symmetric constraints were imposed during geometry optimization. In order to determine the nature of different stationary points on the potential energy surface and to calculate the zero-point vibrational energies (ZPEs), vibrational frequency calculations were also performed using the same level of theory at which the optimization was made. All the stationary points have been characterized as either minima (the number of imaginary frequencies NIMAG = 0) or transition structures (NIMAG = 1). To ensure reliability of the reaction path, intrinsic reaction coordinate (IRC) calculations developed by Gonzalez and Schlegel in the mass-weighted internal coordinate system was used.[28] The binding orientations of $Au\text{-}Ag^-$ with NO and O_2 were studied by observing the SOMO, HOMO and LUMO isosurfaces.

The thermochemical parameters like standard reaction enthalpy (ΔH_r) and Gibbs free energy (ΔG_r) at a temperature T were estimated from the difference of H and G values of products and reactants at that temperature:

$$\Delta H_r(T) = \sum_{prod} (E_0 + H_{corr}) - \sum_{React} (E_0 + H_{corr})$$

$$\Delta G_r(T) = \sum_{prod} (E_0 + G_{corr}) - \sum_{React} (E_0 + G_{corr})$$

where E_0 is the total electronic energy including ZPE and H_{corr} and G_{corr} are the factors to be added to E_0 for getting enthalpy and Gibbs free energy, respectively, at a temperature T for taking into account the contribution of translation, rotation and vibrational motion of a molecule. The H_{corr} and G_{corr} are defined as:

$H_{corr} = H_{trans} + H_{rot} + H_{vib} + RT$

$G_{corr} = H_{corr} - TS_{total}$ where entropy; $S_{total} = S_{trans} + S_{rot} + S_{vib} + S_{el}$

The thermal zero point energy correction (TZPE) is the thermal correction to the internal energy at 298 K.

3. Results and discussion

3.1 Reliability of the method

Previous investigations[17,29-33] showed that the B3LYP functional is sufficiently accurate for describing noble-metal systems. To further verify the reliability of our methods, we also calculated the bond lengths for Au-Ag^-, NO and O_2 and dissociation energy calculations for Au-Ag^- and NO to compare the corresponding experimental values. As shown in Table 1, our calculated values B3LYP level for bond lengths and dissociation energies are in a reasonable agreement with the corresponding experimental results.[30,34,35] However, to check the additional accuracy for interaction of NO and O_2 with the metal species, we have also compared the bond lengths and dissociation energies for AgO, AuO and AgN with the previous results.[35-38] These results are found to be in good agreement with the previously reported data as recorded in Table 1. Therefore, we come to the conclusion

that the level of theory selected in our study is capable of describing the systems accurately and precisely.

In order to access the multi-reference characteristics, we have performed the T1 diagnostic[39] at CCSD(T) level of theory for transition states and results are given in Table 2. We have found that the calculated T1 diagnostic values are considerably lower than 0.045. It has been established that a T1 value larger than 0.045 indicates a significant multi-reference character.[40] Therefore, we can conclude that the transition states reported in this work do not present a multi-reference character. The thermochemical studies have been performed to analyze the stability of all the species involved in the reactions. The reaction enthalpy (ΔH_r) values show that the reaction is significantly exothermic in nature and thus thermodynamically facile. The ΔH_r obtained amount to be -2.87 eV at 298 K. The calculated free energy (ΔG_r) value of -3.07 eV reveals that the reaction is spontaneous in nature.

3.2 Complexes of Au-Ag$^-$ with O_2 and NO

The formation of complexes between Au-Ag$^-$ with O_2 and NO are depicted in Fig.1. In these calculations, we have considered various possible geometries where the O_2 and NO molecules approach the dimer with different orientations as well as different possible spin combinations between the dimer with O_2 and NO molecule. The most stable structures are shown in Fig. 1. For O_2 adsorption (Table S1 of supplementary information), the other two possible orientations leading to dissociative adsorption are found to be less favorable energetically having lower values of binding energies. Similarly, for NO adsorption also, we optimized one additional orientation by combining N atom together with both Au and Ag atoms. But this structure possessed binding energy value 0.08 eV only which is much smaller compared to the side bonded orientation. The less favorable orientations are not considered during the present study. The preferred orientations are identical with that of O_2 and CO

binding to Au_2^- dimer as reported earlier.[9] Following the previous catalytic studies of our group,[8,41] for the catalyst Au-Ag^-, we checked the stable structure by varying the spin multiplicity and found that the doublet system is most stable. The energies for the quartet and sextet structures are quite high compared to doublet structures as reported in Table S2 of the supplementary information. Hence we have taken the doublet Au-Ag^- structure as consideration for the whole reaction. For Au-Ag^- dimer, O_2 can bind to Ag or Au site, forming complex $AuAg^-$-O_2 or $AgAu^-$-O_2. The calculated binding energies are 1.733 and 1.162 eV for these two complexes, respectively. This indicates that O_2 prefers to bind to Ag-site of $AuAg^-$ similar to the previous study.[17] This fact was further confirmed by calculated longer O-O distance (1.390 Å) in $AuAg^-$-O_2 than that in $AgAu^-$-O_2 (1.373 Å) which are in close agreement with previous reported values.[17] The amount of electron transfer from the dimer to O_2 in these two complexes is 0.645 e in $AuAg^-$-O_2 and 0.557 e in $AgAu^-$-O_2. The transferred electrons enter the π^* orbital of O_2 to reduce O-O bond strength. While more electrons are transferred, the larger the O-O distances in $AuAg^-$-O_2. Similarly, for the complexes of $AuAg^-$ with NO, our calculations show that the binding energies of NO over the Ag and Au sites are 0.775 and 0.562 eV, respectively. This reveals that the Ag-site of $AuAg^-$ is also more active toward NO binding than the Au-site. For binding of O_2 and NO with $AuAg^-$ too, we have considered different spin multiplicities (Table S2 of the supplementary information) and choose the most stable one for this study. The spin densities for different species are also calculated to support our spin states and provided in Table S3.

On comparing the relative stability of the complexes of $AuAg^-$ with O_2 to those with NO, we see that the interaction of $AuAg^-$ with O_2 is stronger than that with NO. This is also confirmed by the geometrical parameters shown in Fig. 1. From the figure, it can be seen that the O-O distance in $AuAg^-$-O_2 is increased by 14.9% compared to that in isolated O_2, while

the N-O distance in $AuAg^-$-NO is only increased by 9.0% compared to that in isolated NO, indicating a stronger interaction of $AuAg^-$ with O_2 than with NO. Also, it is clear from Fig. 2 that the SOMO, HOMO and LUMO isosurfaces of Au-Ag^-, O_2, and NO clearly match with shapes and symmetries. It further explains the binding orientations of NO with Au-Ag^- similar to O_2.

In the following sections, we discuss the detailed reaction mechanism of the NO oxidation over Au-Ag^- for both Ag and Au sites, from which we expect to provide some information regarding the catalytic activity of Au-Ag^- dimer as well as priority of the two metal sites for NO oxidation. Optimized geometries of reactants, intermediates, transition states and products obtained at the DFT level using B3LYP functional are shown in Fig. 3 for both Ag and Au sites. Transition states searched on the potential energy surfaces of pathways (I-II) are characterized as TS1, TS2 and TS3, respectively. This search was made along the minimum energy path on a relaxed potential energy surface.

3.3. NO oxidation along Ag sites of Au-Ag^- dimer

The formation of complexes of Au-Ag^- with O_2 and NO molecules is expected to be the initial step of NO oxidation. Path I start from the adsorption of NO with the Au-Ag^- dimer. After this adsorption, the attack of upcoming O_2 molecules gives IM1 which lies below the reactant by 2.24 eV. Subsequently, another NO molecule attacks IM1 to give IM2 which involves with O-N-O-O-N-O like species. From IM2, we get two NO_2 molecules simultaneously via TS1 which involves a O-N-O-O-N-O group (Fig.3). Calculated geometrical parameters of TS1 clearly indicate that the O-O bond is weakening and the N-O bond is forming. Visualization of the optimized structure of TS1 further reveals the elongation of O-O bond length from 1.506 to 1.573 Å with a simultaneous shrinkage of the N-O bond from 1.292 to 1.242 Å. In the optimized geometry of TS1, NO abstracts an O atom

to produce NO_2 and complete the cycle. All the structures except the TS1 associated with only real vibrational frequencies. But TS1 confirms its existence with an imaginary frequency of 568i cm^{-1}.

For pathway II, similar to the pathway III of our previous study,[32] the initial step is the adsorption of O_2 molecule with Au-Ag^- to give a preadsorbed superoxo like species Au-Ag^--O_2. The first NO molecule then attack this species to give IM3 which lies below the reactants by 2.67 eV. From IM3, we get IM4 via TS2 (Fig. 3) which involves a O-O-N-O group and associated with an imaginary frequency of 396i cm^{-1}. In this step one NO_2 molecule is released. The attack of second NO molecule on IM4 results IM5. From IM5, second NO_2 molecule is released via TS3 (Fig.3) which possesses an imaginary frequency of 140i cm^{-1}. Calculated geometrical parameters of TS2 and TS3 indicate that the O-O and Ag-O bonds are weakening and the O-N bond is forming. Similar analysis made on the optimized structure of TS2 and TS3 reveals the elongation of O-O bond lengths from 1.484 to 1.549 Å and shrinkage of N-O bond lengths from 1.416 to 1.331 Å in case of TS2 and elongation of Ag-O bond length from 2.176 to 2.182 Å and shrinkage of N-O bond lengths from 1.355 to 1.352 Å in case of TS3, respectively. To verify the formation of transition states, we calculate the IRC paths for both the pathways. The IRC plots for transition states reveal that the transition state structures connect smoothly the reactant and the product sides. The energies of reactants, transition states and products obtained in the IRC calculations are in excellent agreement with the individually optimized values at both the levels of theory.

In the next step, we construct schematic potential energy surfaces of the titled reaction obtained for both the pathways at the B3LYP + ZPE levels to search the most dominant path of the reaction (Fig.4) In the construction of energy diagram, zero-point corrected total energies are utilized. These energies are plotted with respect to the ground

state energy of reactants (Au-Ag^- +O_2/NO) arbitrarily taken as zero. From Fig. 4, it is clear that Pathway II is the dominant path involving lower barrier height for the NO oxidation promoted by Au-Ag^- dimer. For path II, the step involving TS3 is the rate determining step as indicated by its higher barrier height compared to that of TS2. The barrier heights obtained from the energy profile diagrams are listed in Table 3. In this study, to test the influence of basis set quality we performed single point calculations by using an extended basis set, LANL2TZ(f)[42] on the metal centers. The maximum difference in energy between LANL2DZ and LANL2TZ(f) levels was found to be 0.37 eV (Table S4 of supplementary information) with percentage error less than 0.1 %. Therefore, the LANL2DZ basis set used in this work is suitable and accurate for computation.

3.4. NO oxidation along Au sites of Au-Ag- dimer

Both the reaction pathways are carried out for the Au sites of Au-Ag^- dimer as well. The energy profile diagram for Au site is shown in Fig. 5. For pathway I, TS4 involves with an imaginary frequency of 571i cm^{-1}. Visualization of the optimized structure of TS4 further reveals the elongation of O-O bond length from 1.457 to 1.578 Å with a simultaneous shrinkage of the N-O bond from 1.485 to 1.454 Å. In the optimized geometry of TS4, NO abstracts an O atom to produce NO_2 and complete the cycle. The barrier height for this pathway is found to be 1.68 eV.

Similarly for pathway II, TS5 and TS6 are associated with imaginary frequencies of 360i cm^{-1} and 171i cm^{-1}, respectively. Calculated geometrical parameters of TS5 and TS6 indicate that the O-O and Au-O bond are weakening and the O-N bond is forming. Similar analysis made on the optimized structure of TS5 and TS6 reveals the elongation of O-O bond length from 1.486 to 1.528 Å and shrinkage of N-O bond length from 1.439 to 1.386 Å in case of TS5 and elongation of Au-O bond length from 2.196 to 2.203 Å and shrinkage of N-

O bond length from 1.359 to 1.351 Å in case of TS6, respectively. The bond length between Au-O(2.061 Å) in IM6 is comparable to Au-O bond length(1.990 Å) of Au_2^--O of our previous study.[32] The barrier heights obtained from the energy profile diagram are shown in Table 3. Here also, to verify the formation of TS, we calculated the IRC paths for both the pathways. The IRC plots for transition states reveal that the transition state structure connects smoothly the reactant and the product sides. The energies of reactants, transition states and products obtained in the IRC calculations are in excellent agreement with the individually optimized values at both the levels of theory.

From the above results, we come to the conclusion that for both Au and Ag sites of Au-Ag^--dimer, pathway II is more dominant compared to pathway I as indicated by its lower barrier height in both the cases. However, when we compare the reactions in both the sites, it clearly indicates the preference of Au site compared to Ag site for NO oxidation (from the comparison of energy barriers of Table 3) in Au-Ag^--dimer. This is in accordance with the previous report[17] that the Au site is more active than the Ag site for $AuAg^-$ dimer towards CO oxidation. This result strongly suggests that like CO oxidation, the anionic Au-Ag^-dimer shows catalytic activity towards NO oxidation as well.

4. Conclusions

We present here the potential energy profile (including geometries, energies and vibrational frequencies of reactant, intermediates, transition states and products) and thermochemical data for the oxidation of NO to NO_2 promoted by gold-silver anionic dimer investigated at the DFT level of theory. The reaction is explored with two possible pathways. For Au-Ag^- dimer, the Au site is more active than the Ag site, and the calculated energy barrier values for rate determining step for the Au-site catalytic reaction are remarkably

smaller than that for the Ag-site catalytic reaction. Energetic calculation reveals that the most dominant oxidation pathway is the Path II involving O-O-N-O group. We hope that our present theoretical studies may give useful information on the reaction mechanism and can provide powerful guidelines for future experimental studies for the title reaction. It will provide valuable information for understanding the higher catalytic activity of Au-Ag nanoparticles for NO oxidation than either pure metallic catalyst.

Acknowledgements

The work is funded by the Department of Science and Technology, New Delhi in the form of a research project (SR/NM/NS-1023/2011-G). DB is thankful to the Council of Scientific and Industrial Research, New Delhi for providing Senior Research Fellowship. The financial support in the form of Dr. D. S. Kothari Post doctoral fellowship to BKM from UGC, New Delhi is also acknowledged. We are also thankful to the reviewers for their constructive suggestions to improve the quality of the manuscript. Special thanks to Franck Rabillood, Université de Lyon, France for providing useful suggestions.

References

1 P. Granger, C. Dujardin, J.-F. Paul, G. Leclercq, *J. Mol. Catal. A: Chem*., 2005, **228** 241-253.

2 P.L. Silverston, *Catal. Today,* 1995, **25**, 175-194.

3 V.I. Pârvulescu, P. Grange, B. Delmon, *Catal. Today,* 1998, **46**, 233-316.

4 R.M. Heck, R.J. Farrauto, *Appl. Catal. A: Gen,* 2001, **221**, 443-457.

5 R. Burch, J.P. Breen, F.C. Meunier, *Appl. Catal. B: Environ.,* 2002, **39**, 283-303.

6 G.I.C. Jiron, C. Gonzalez, J. Benavides, *J. Phys. Chem. C,* 2012, **116,** 16979-16984.

7 R.B. Getman, W. F. Schneider, *Chem. Cat. Chem.,* 2010, **2**, 1450-1460.

8 B. Kalita, R. C. Deka, *J. Am. Chem. Soc.*, 2009, **131**, 13252-13254.

9 H. Hakkinen, U. Landman, *J. Am. Chem. Soc*., 2001, **123**, 9704-9705.

10 D. Torres, S. González, K.M. Neyman, F. Illas, *Chem. Phys. Lett*., 2006, **422**, 412-416.

11 X.L. Ding, Z. Li, J. Yang, J.G. Hou, Q. Zhu, *J. Chem. Phys*., 2004, **121**, 2558.

12 L.D. Socaciu, J. Hagen, T.M. Bernhardt, L. Woste, U. Heiz, H. Hakkinen, U. Landman, *J. Am. Chem. Soc*., 2003, **125**, 10437-10445.

13 Y. Gao, N. Shao, Y. Pei, Z. Chen, X. C. Zeng, *ACS Nano*, 2011, **5**, 7818-7829.

14 M.A. Tafoughalt, M. Samah, *Physica B*, 2012, **407**, 2014-2024.

15 S. Zhao, W. Lu,Y. Ren, Y.Ren, J. Wang, W. Yin, *Comput. Theor. Chem*., 2012, **993**, 90-96.

16 S.L. Peng, L.Y. Gan, R.Y. Tian, Y.J. Zhao, *Comput. Theor. Chem*., 2011, **977**, 62-68.

17 P. Liu, K. Song, D. Zhang, C. Liu, *J. Mol. Model*., 2012, **18**, 1809-1818.

18 V. Stamenkovic, B.S. Mun, K.J.J. Mayrhofer, P.N. Ross, N.M. Markovic, J. Rossmeisl, J. Greeley, J.K. Norskov, *Angew. Chem. Int. Ed,.* 2006, **45**, 2897-2901.

19 W. Song, A.P.J. Jansen, E.J.M. Hensen, *Farad. Discuss*., 2013, **162**, 281-292.

20 L. Zhao, X. Li, C. Hao, C.L. Raston, *Appl. Catal. B: Environ*., 2012, **117**, 339-345.

21 R. Valero, J.R.B. Gomes, D.G. Truhlar, F. Illas, *J. Chem. Phys*., 2010, **132**, 104701.

22 W. Song, E.J.M. Hensen, *Catal. Sci. Technol*., 2013, **3**, 3020-3029.

23 M.J. Frisch, G.W. Trucks, H.B. Schlegel, G.E. Scuseria, M.A. Robb, J.R. Cheeseman, G. Scalmani, V. Barone, B. Mennucci, G.A. Petersson, H. Nakatsuji, M. Caricato, X. Li, H.P. Hratchian, A.F. Izmaylov, J. Bloino, G. Zheng, J.L. Sonnenberg, M. Hada, M. Ehara, K. Toyota, R. Fukuda, J. Hasegawa, M. Ishida, T. Nakajima, Y. Honda, O. Kitao, H. Nakai, T. Vreven, J.A. Montgomery Jr., J.E. Peralta, F. Ogliaro, M. Bearpark, J.J. Heyd, E. Brothers, K.N. Kudin, V.N. Staroverov, R. Kobayashi, J. Normand, K. Raghavachari, A. Rendell, J.C. Burant, S.S. Iyengar, J. Tomasi, M. Cossi, Rega, N.J. Millam, M. Klene, J.E. Knox, J.B. Cross, V. Bakken, C. Adamo, J. Jaramillo, R.E. Gomperts, O. Stratmann, A.J. Yazyev, R. Austin, C. Cammi, J.W. Pomelli, R. Ochterski, R.L. Martin, K. Morokuma, V.G. Zakrzewski, G.A. Voth, P. Salvador, J.J. Dannenberg, S. Dapprich, A.D. Daniels, O. Farkas, J.B. Foresman, J.V. Ortiz, J. Cioslowski, D.J. Fox, Gaussian Inc., Gaussian 09, Revision A. 08, Wallingford, CT, 2009.

24 A.D. Becke, *J. Chem. Phys*., 1992, **96**, 2155.

25 C. Lee, W. Yang, R.G. Parr, *Phys. Rev. B*, 1988, **37**, 785-789.

26 P.J. Hay, W.R. Wadt, *J. Chem. Phys*., 1985, **82**, 270.

27 P.J. Hay, W.R. Wadt, *J. Chem .Phys.,* 1985, **82**, 299.

28 C. Gonzalez, H.B. Schlegel, *J. Chem. Phys.,* 1989, **90**, 2154

29 H.-Q Yang, S. Qin, S Qin, C. –W. Hu, *J. Comput. Chem.,* 2009, **30**, 847-863.

30 D.Y. Wu, B. Ren, Y. X. Jiang, X. Xu, Z.Q. Tian, *J. Phys. Chem. A,* 2002, **106**, 9042-9052.

31 T. Yoneda, T. Takido, K. Konuma, *Appl. Catal. B: Environ*., 2008, **84**, 667-677.

32 R.C. Deka, D. Bhattacharjee, A.K. Chakrabartty, B.K. Mishra, *RSc. Adv.,* 2014, **4**, 5399-5404.

33 D. Bhattacharjee, B.K. Mishra, A.K. Chakrabartty, R.C. Deka, *Comput. Theor. Chem.,* 2014, **1034**, 61-72.

34 J.C. Fabi, J.D. Langenberg, Q.D. Costello, M.D. Morse, L. Karlsson. *J. Chem. Phys*., 2001, **115**, 7543

35 K.P. Huber, G. Herzberg, Constants of Diatomic Molecules, Van Nostrand Reinhold, New York, 1979.

36 B. Yoon, H. Ha1kkinen, U. Landman, *J. Phys. Chem. A,* 2003, **107**, 4066.

37 A. Martínez, *J. Braz. Chem. Soc.,* 2005, **16**, 337.

38 D. R. Lide, CRC Handbook of Chemistry and Physics, Internet Version 2005, <http://www.hbcpnetbase.com>, CRC Press, Boca Raton, FL, 2005.

39 T.J. Lee, P.R. Taylor, *Int. J. Quantum Chem., Quant. Chem. Symp.,* 1989, **S23**, 199-207.

40 S.R. Miller, N.E. Schultz, D.G. Truhlar, D.G. Leopold, *J. Chem. Phys*., 2009, **130**, 024304.

41 S. Baishya, R. C. Deka, *Int. J. Quantum Chem.,* 2014, **114**, 1559.

42 L. E. Roy, P. J. Hay, R. L. Martin, *J. Chem. Theory Comput.,* 2008, **4**, 1029.

Table 1: Calculated and experimental bond lengths, d (in Å) and dissociation energies, D.E. (in eV) at B3LYP level

Methods	d (Å)			D.E. (eV)		
	$Au\text{-}Ag^-$	O_2	NO	Au-Ag	O_2	
B3LYP	2.771	1.206	1.148	1.81	5.29	
Experimental	2.772[a]	1.209[b]	1.151[c]	2.08±0.1[a]	5.12[c]	
	AgO	AuO	AgN	AgO	AuO	AgN
B3LYP	2.074	1.924	2.214	1.49	1.45	1.44
Experimental	2.0[c]	1.96-1.99[d]	2.11[e]	2.21±0.21[f]	2.23±0.21[f]	

[a]Ref. [34], [b]Ref. [31], [c]Ref. [35], [d]Ref. [36], [e]Ref. [37], [f]Ref. [38]

Table 2: T1 diagnostic values of the transition states for Ag and Ag sites of Au-Ag^--dimer using B3LYP functional.

Ag site	TS1	TS2	TS3
	0.032	0.025	0.023
Au site	TS4	TS5	TS6
	0.029	0.026	0.024

Table 3: Calculated barrier heights for both pathways along Ag and Au sites of Au-Ag$^-$-dimer at B3LYP level.

Reaction Sites	Energy Barriers (eV)		
	Pathway I	Pathway II	
Ag site	2.13	1.37	0.95
Au site	1.68	1.41	0.17

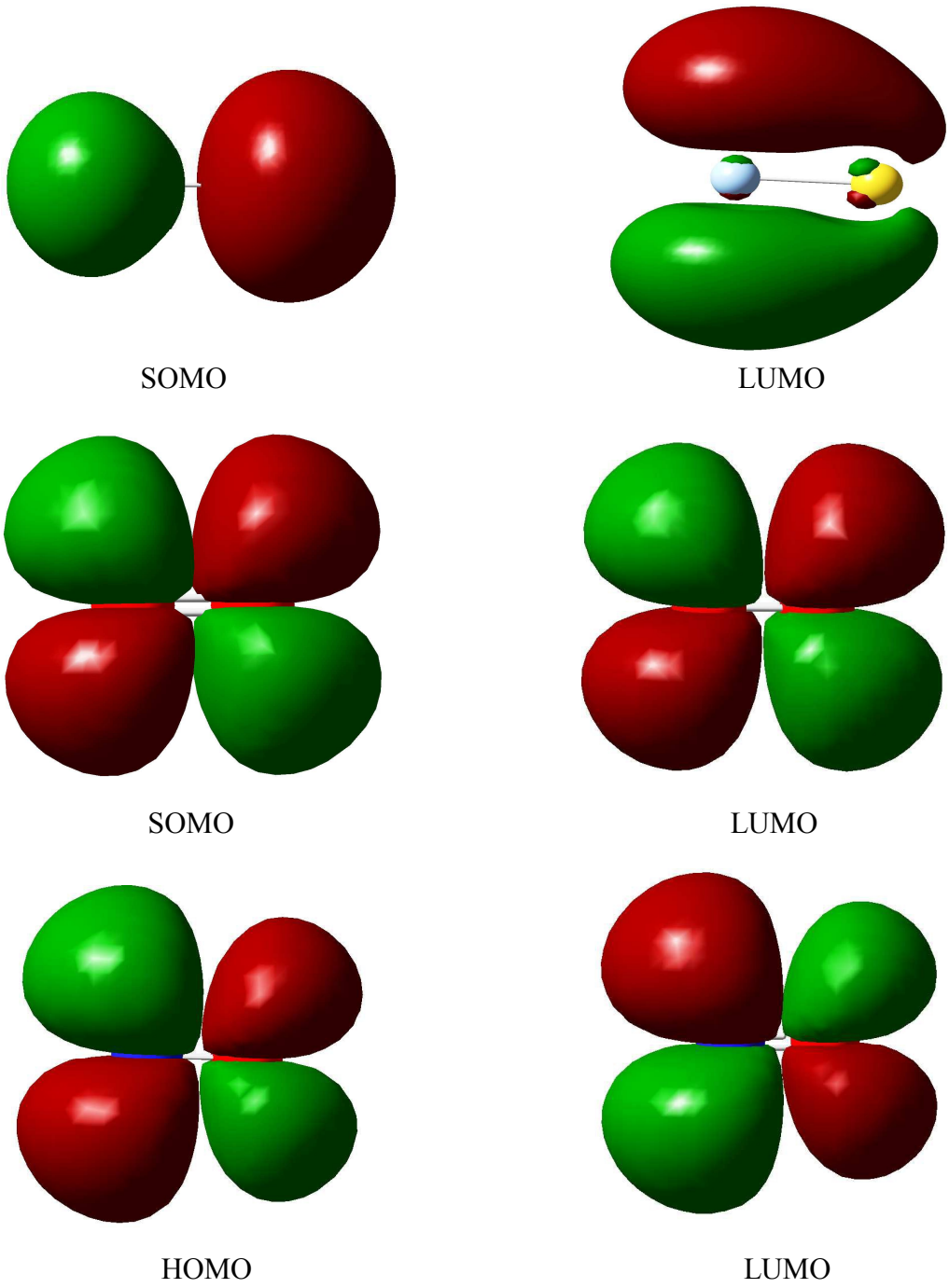

Fig. 1. The SOMO, HOMO and LUMO isosurfaces for Au-Ag^- dimer, O_2 and NO molecules.

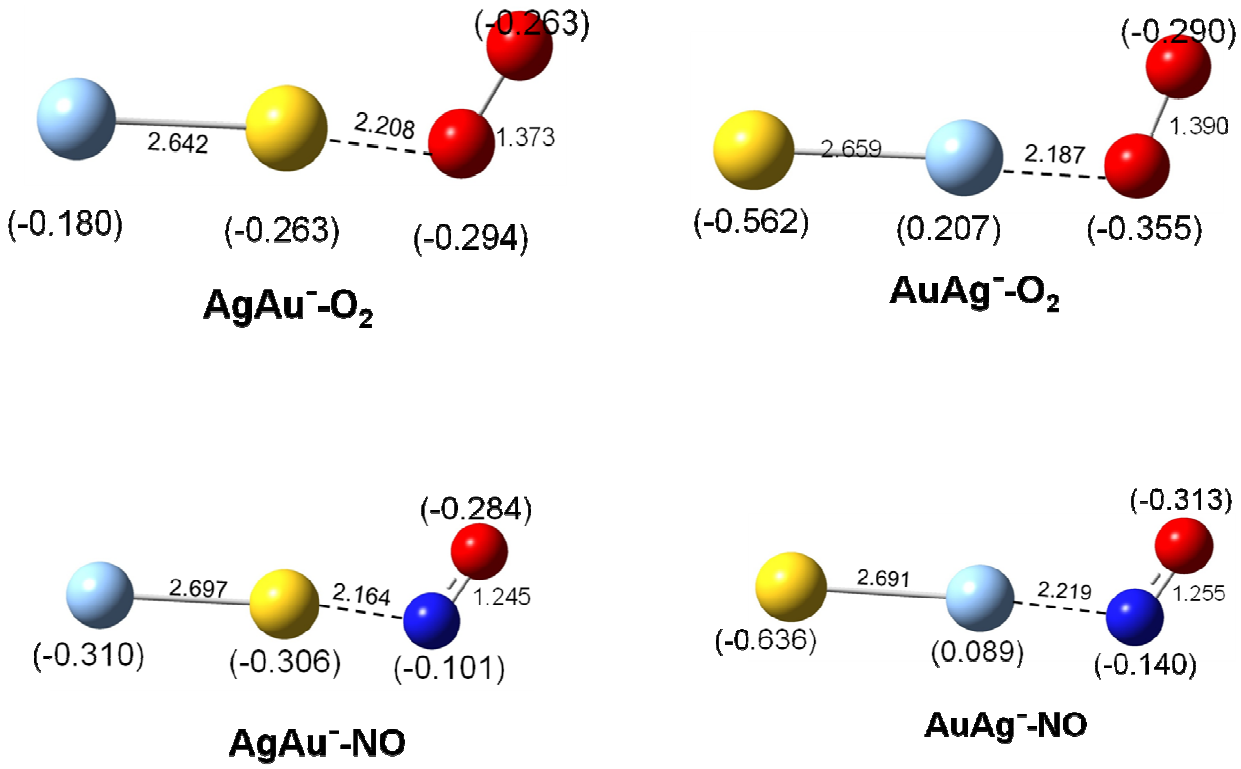

Fig. 2. Optimized geometries for complexes between O_2 and NO molecules with Au-Ag-dimers in two different sites. The numbers in parentheses are calculated natural charges of atoms (in e). (Gold in yellow, Ag in sky blue, oxygen in red and nitrogen in dark blue colors)

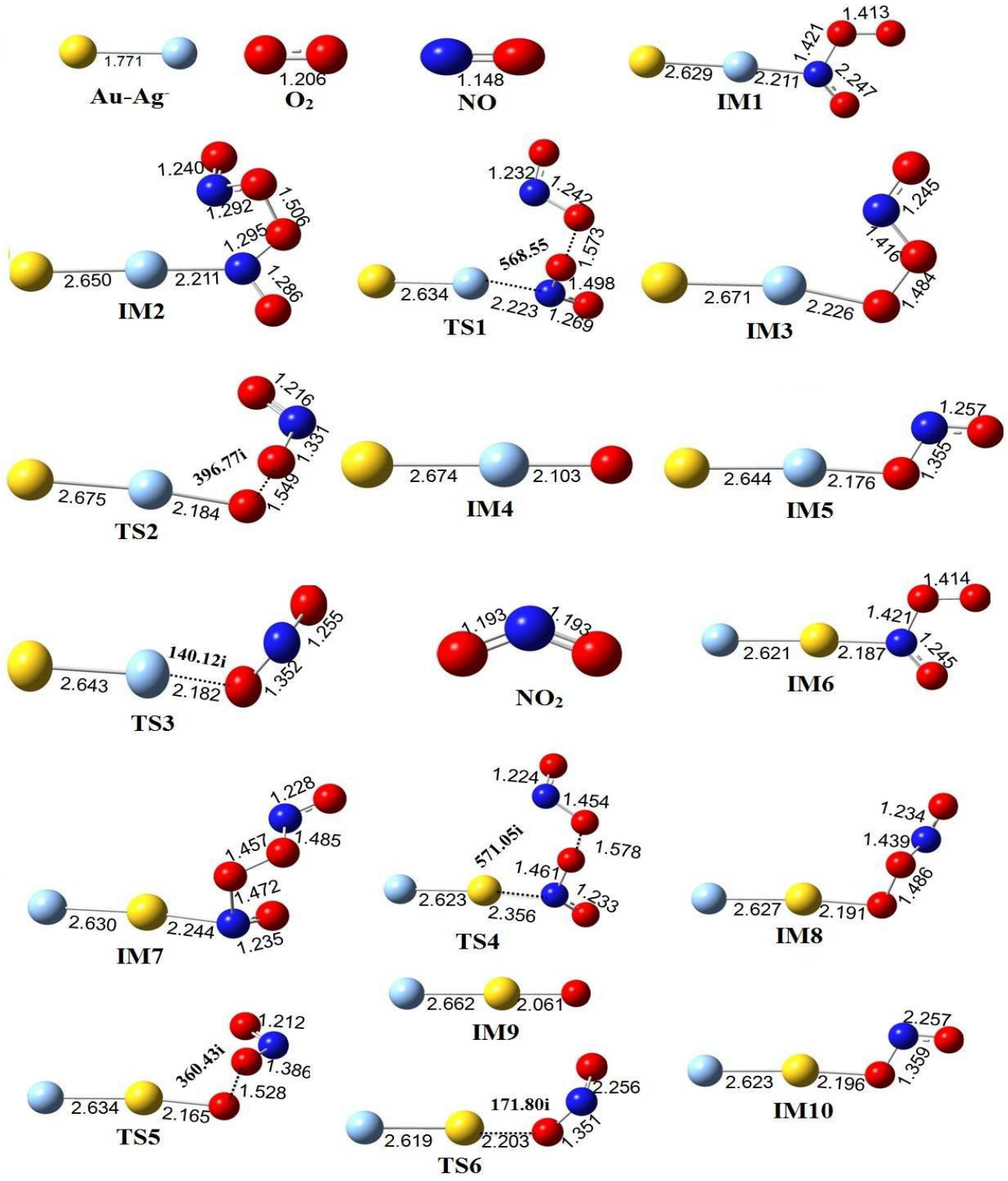

Fig. 3. Optimized geometries of reactants, intermediates, transition states and products involved in the oxidative pathways of NO by Au-Ag⁻ dimer along Ag and Au sites.

(Gold in yellow, Ag in sky blue, oxygen in red and nitrogen in dark blue colors)

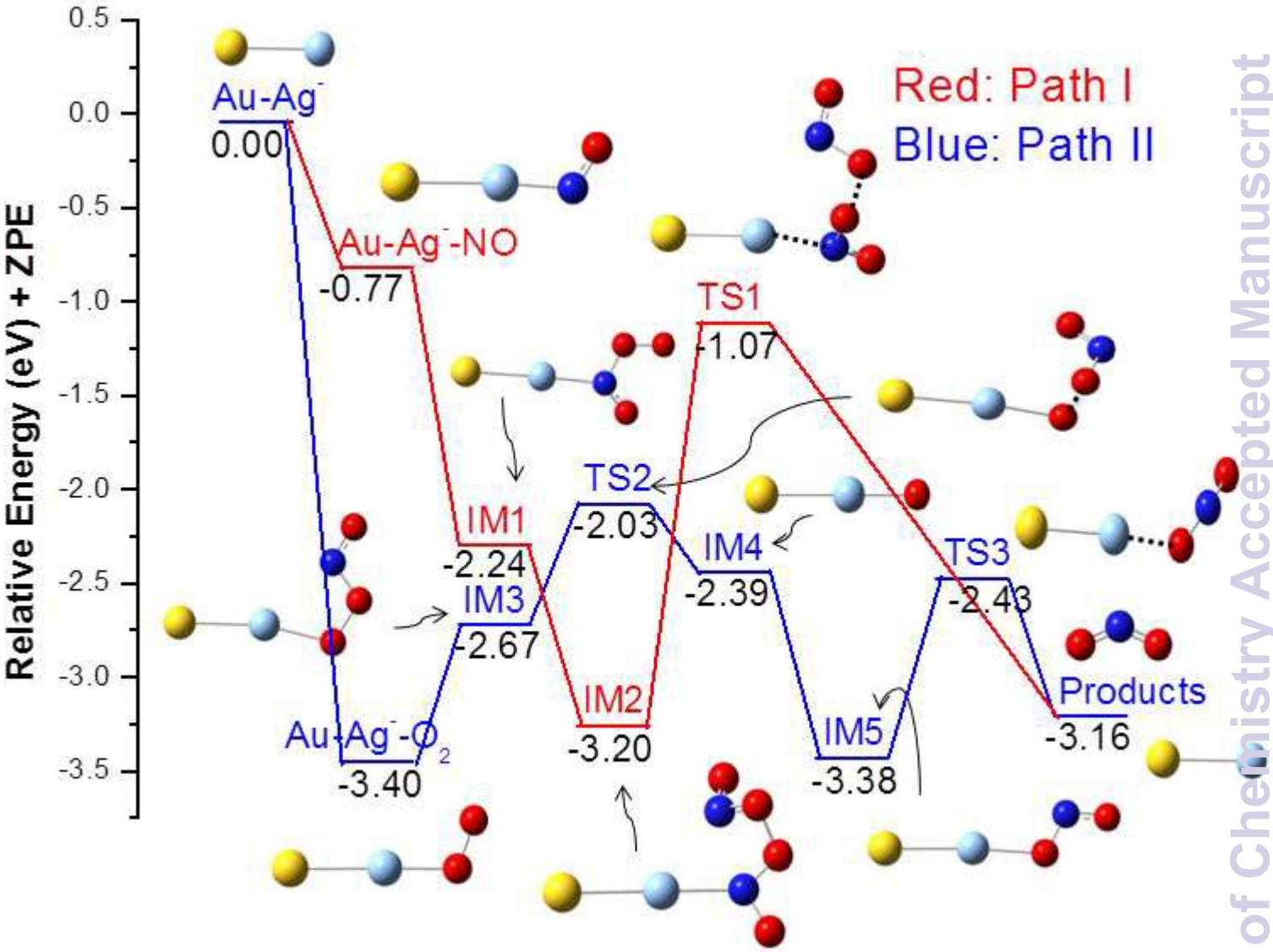

Fig. 4. Relative energy profile for the NO oxidation by Au-Ag⁻ dimer along Ag site.

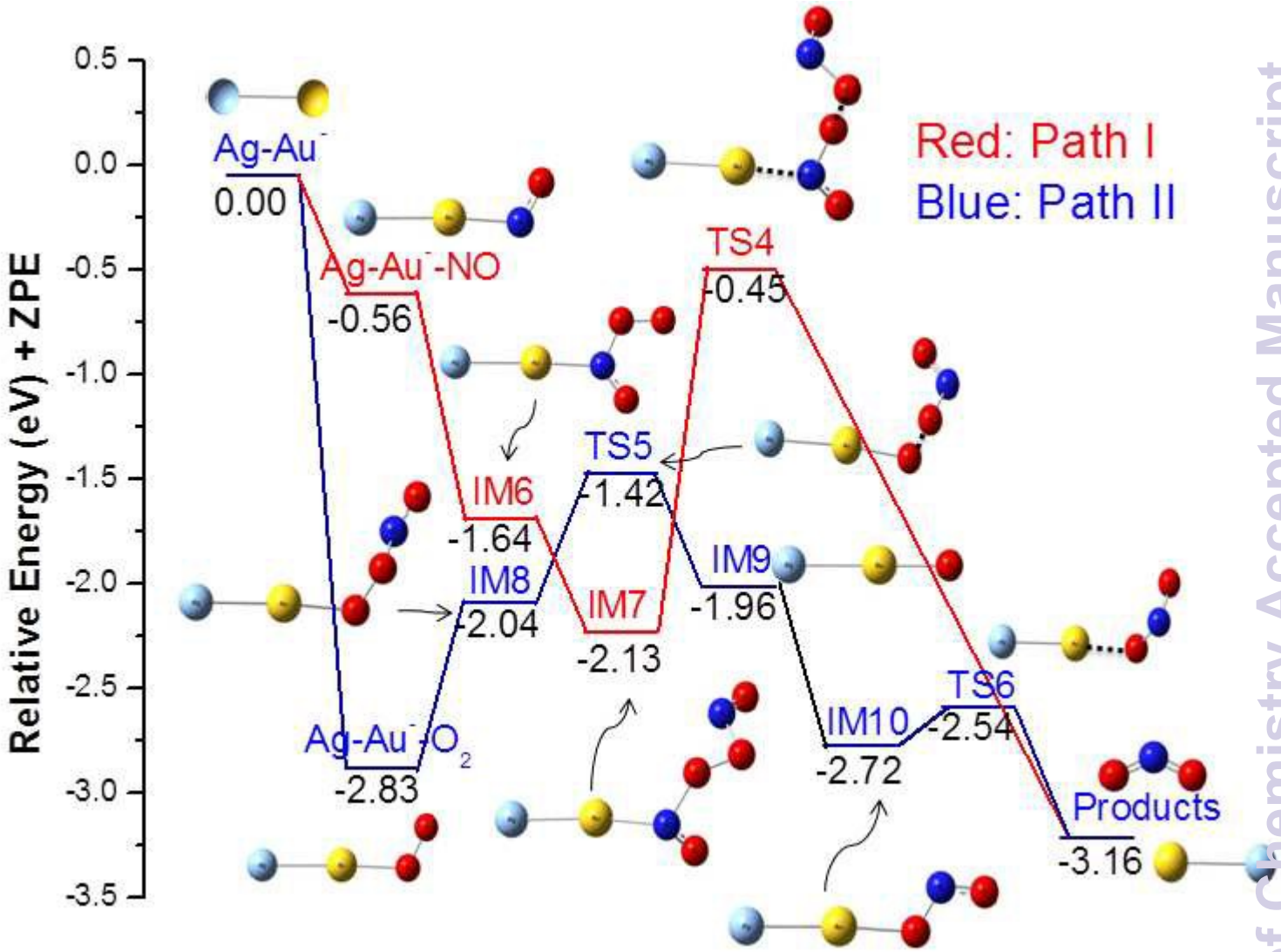

Fig. 5. Relative energy profile for the NO oxidation by Au-Ag⁻ dimer along Au site.